Hi-fidelity multi-scale local processing for visually optimized far-infrared Herschel images

G. Li Causi, E. Schisano, S. J. Liu, S. Molinari, A. Di Giorgio

G. Li Causi, E. Schisano, S. J. Liu, S. Molinari, A. Di Giorgio, "Hi-fidelity multi-scale local processing for visually optimized far-infrared Herschel images," Proc. SPIE 9904, Space Telescopes and Instrumentation 2016: Optical, Infrared, and Millimeter Wave, 99045V (29 July 2016); doi: 10.1117/12.2233241

SPIE.

Event: SPIE Astronomical Telescopes + Instrumentation, 2016, Edinburgh, United Kingdom

Hi-fidelity multi-scale local processing for visually optimized far-infrared Herschel images

Li Causi G.*[a], Schisano E.[a], Liu S. J. [a], Molinari S.[a], Di Giorgio A.[a]
[a]INAF-Istituto di Astrofisica e Planetologia Spaziali, Via Fosso del Cavaliere 100, Roma, Italia

ABSTRACT

In the context of the "Hi-Gal" multi-band full-plane mapping program for the Galactic Plane, as imaged by the Herschel far-infrared satellite, we have developed a semi-automatic tool which produces high definition, high quality color maps optimized for visual perception of extended features, like bubbles and filaments, against the high background variations. We project the map tiles of three selected bands onto a 3-channel panorama, which spans the central 130 degrees of galactic longitude times 2.8 degrees of galactic latitude, at the pixel scale of 3.2", in cartesian galactic coordinates. Then we process this image piecewise, applying a custom multi-scale local stretching algorithm, enforced by a local multi-scale color balance. Finally, we apply an edge-preserving contrast enhancement to perform an artifact-free details sharpening. Thanks to this tool, we have thus produced a stunning giga-pixel color image of the far-infrared Galactic Plane that we made publicly available with the recent release of the Hi-Gal mosaics and compact source catalog.

Keywords: Multi-scale image processing, adaptive contrast, local color balance, visual rendering, far infrared

1. INTRODUCTION

Astronomical images are commonly characterized by a very high "dynamic range" at any scale, which means that the features brightness changes by orders of magnitudes both among adjacent locations and between distant areas. When different wavelength bands are joined into an rgb color image, they also usually show quite different intensities and different pixel scales. All that may lead to unclear pictures, unable to unambiguously display to the eye all the information they contain unless a suitable processing is applied.

In this work, we present the multi-scale local stretching and color balancing algorithms we developed with the aim to produce a high-fidelity color rendition of the multi-band far-infrared (FIR) maps of the Galactic Plane survey, acquired with the Herschel space observatory[1] within the Hi-Gal project[2]. The scope of such processing is twofold: for the outreach, we need to release "eye-catching stunning images" where the relevant features like bubbles, filaments, pillars, are recognizable in a clear and sharp way; while for science, a visually optimized image allows us to directly compare multi-band information for bright and faint regions simultaneously.

2. INITIAL PROCESSING

2.1 The Hi-GAL survey

Hi-GAL, the Herschel infrared GALactic plane survey[2], is the keystone of a suite of continuum Galactic Plane surveys from the near infrared to the radio, and covers five wavebands centered at 70, 160, 250, 350 and 500μm, respectively, encompassing the peak of the spectral energy distribution of cold dust with temperature in the range $8 \leq T \leq 50$K. The observations were acquired by subdividing the surveyed area into square tiles of 2.2° in size to obtain a complete coverage of a $|b| < 1°$ strip, following the IRAS distribution of sources on the Galactic Plane. Each tile was observed in five bands simultaneously, with the PACS[3] and SPIRE[4] Herschel bolometer array cameras in parallel mode, with a ~20' offsets in the fields of view of the two instruments. The maps were observed twice, along two orthogonal scan directions, subsequently combined via software.

The reduction of the raw data has been carried out using the software ROMAGAL[5] and UNIMAP[6], whose output is a 32-bit depth photometric image for each band and tile, mapped on a cartesian pixel grid with a sampling of 3.2", 4.5",

*gianluca.licausi@inaf.it

Space Telescopes and Instrumentation 2016: Optical, Infrared, and Millimeter Wave, edited by Howard A. MacEwen, Giovanni G. Fazio, Makenzie Lystrup, Proc. of SPIE Vol. 9904, 99045V · © 2016 SPIE · CCC code: 0277-786X/16/$18 · doi: 10.1117/12.2233241

6.0”, 8.0”, and 11.5” respectively in each band. The maps are absolutely calibrated, following the procedure described in Bernard et al. 2010[7], and then stitched in couples, with the aim to remove some reconstruction artifacts that appears at tile borders, in the regions covered by a single scan direction. Such “two-tiles” mosaics (see Figure 1), coming in FITS format[8], are the input to the work described here, which, in this first release, is restricted to the inner Galaxy regions, between $60° \geq l \geq -70°$, and to the three bands from 70μm to 250μm. We implemented the process in a custom code in IDL language[9].

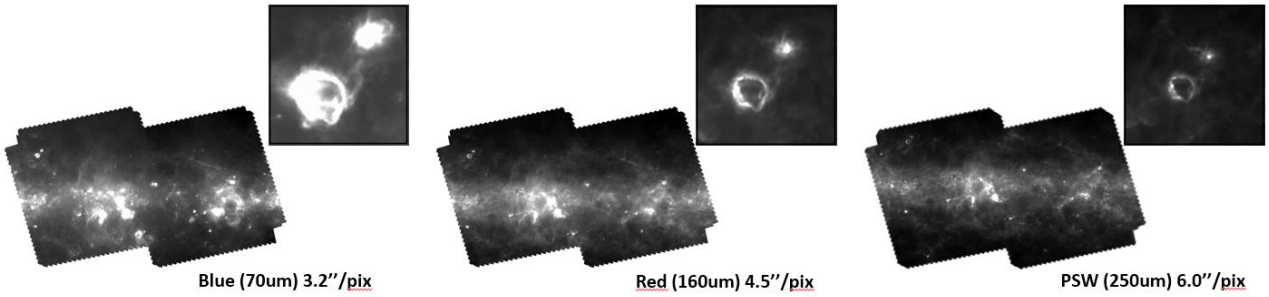

Figure 1: “Two-tiles” mosaics of the same region in the three selected bands centered at 70, 160, 250μm, and called “Blue”, “Red”, and “PSW”, respectively. The top-right inserts enlarge the same region by displaying three boxes with the same number of pixels per side, thus showing the different resolution for the different bands.

2.2 Pre-processing steps

To ensure the use of uniformly calibrated maps, a set of preprocessing steps has been defined and implemented in specifically developed procedures.

Given that the highest resolution, for the 70μm band, is 3.2”/pixel (see Figure 1), and that the full Galactic Plane will need a 360°×3.8° cylindrical map, taking into accout the Milky Way warp, we compute that the complete 32-bit three-channels map will cover a $\sim 4 \cdot 10^5 \times 4 \cdot 10^3 \approx 1.7$ Gpix image, spanning ~20.8 Gb of memory.

In order to manage such huge array, we chose to store the image in a BigTIFF format file[10], which we memory-map on disk via custom routines based on the `SHMMAP` group of IDL functions, allowing us to easily and rapidly read/write sub-regions of the full image. This format also has the advantage to be a standard for the giga-pixel image viewers, like KrPano[11] and others.

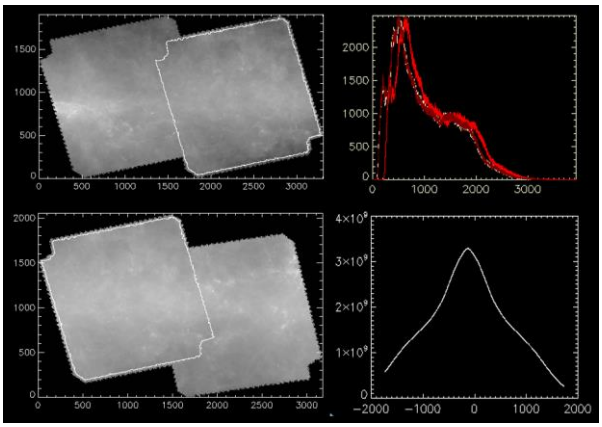

Figure 2: Offset computation for a couple of adjacent tiles, whose overlapping is shown at left; the optimal offset is found maximizing the cross-correlation (bottom-right) of one tile’s histogram (bright red) to the histogram of the other (dark red), as shown in top-right plot.

The first step analyzes all the two-tiles mosaics that intersect the required sky region, and computes the inter-calibration offsets among them. This is needed because the absolutely calibrated two-tile maps show different average offsets which, even if contained within the calibration errors, produce a step-wise background in the final stitched panorama. We thus developed an offset matching procedure that maximizes, for each band independently, the histogram cross-correlation in the overlapping area of each adjacent maps, as depicted in Figure 2.

The second pre-processing step projects all the tiles onto the final 3-channels image array. The developed procedure works piece-wise by firstly cutting the final stripe of the Galaxy panorama in a number of adjacent square regions, named "frames" hereafter, and then bi-linearly interpolating all the involved map tiles to the pixel grid of each frame. The three primary colors red, green and blue, are assigned in this projection to the 250, 160, and 70μm bands, respectively.

During this reading/projection of the input tiles, we also flag each missing data and saturated pixel, thus building a binary flag mask for each of them, which are useful for excluding those pixels from the following processes.

2.3 Dynamic range compression

The merged-channels image so produced is still a linear photometric map, i.e. the gray level across the whole image is linearly proportional to the flux detected in the area of each pixel. This is not yet a visually optimized image, as displayed at top of Figure 3. In this kind of image, if we increase the luminosity to reveal the faint regions we unavoidably saturate the brightest regions. Avoiding saturation is only possible if we alter the global linear relation between the measured flux and the image gray levels. The dynamic range of the Hi-GAL maps, i.e. the ratio between the maximum intensity in the peaks around galaxy center, and the noise level in the darkest regions of the outer Galaxy, is of the order of 10^6. This contrast cannot be coded within the 8-bits per channel of a color image displayed by normal monitors, or printings. The scope of our work has been to remap this wide dynamics within the 8-bits range, without losing the morphological information.

The first non-linear and non-global transformation we do is to fit, for each channel, a low order polynomial to the background level across the whole panorama, to remove the highly variable background along different galactic longitude. Then we normalize the result between a minimum and a maximum threshold (histogram stretching), which we interactively choose on a down-sampled grayscale visualization of each channel. Finally, we apply an inverse hyperbolic sine (asinh) transfer function, which maintains a linear relation for the fainter pixel values, while asymptotically decrease the brightest levels.

Such easy transformations already results in a much more comprehensible visualization, as shown by the third stripe in Figure 3, however it still displays an ubiquitous yellow-greenish color. Such image is still scientifically correct, in the sense that it keeps the information that the median intensity of the 160μm band (assigned to green) is higher than the other bands, Our aim, however, is to improve the visual perception of morphological features, even if not keeping the photometry. Hence we apply a "color balance", that aims to equalize the three channel histograms by scaling each channel in a non-linear way, depending on the values of the other channels thus producing a neutral average color. This process removes the greenish tint from our image, leading to the bottom stripe of Figure 3.

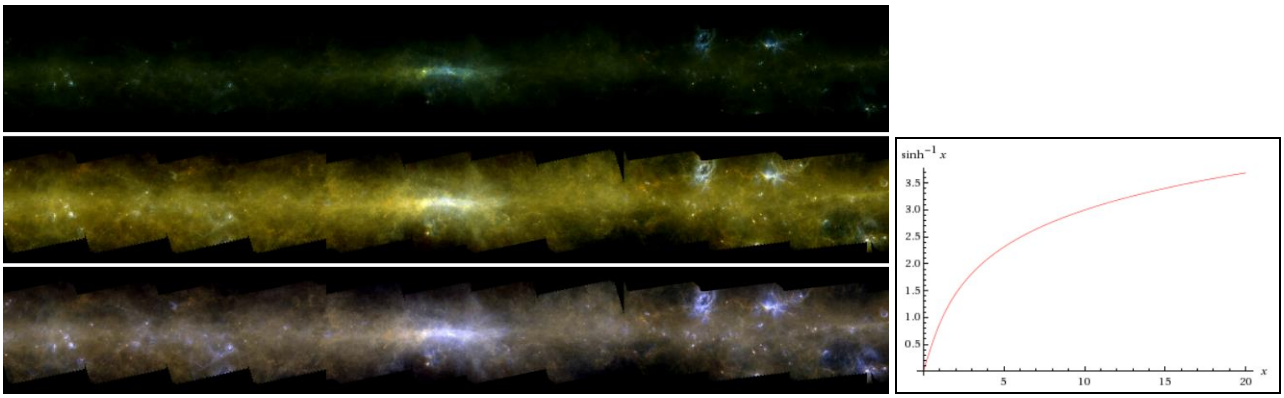

Figure 3: Left panels: central piece of the linear intensity merged image (top) compared to its asinh transformation after polynomial background subtraction (middle), and after a color balance (bottom). Right panel: a plot of the asinh transfer function.

3. MULTI-SCALE LOCAL PROCESSES

3.1 Adaptive histogram stretching and color balance

The image resulting after these global processes is still far from our goal. In fact, as clearly shown in Figure 4, left panel, all the features have a very similar color and brightness, and the dust filaments are not recognizable at a first glance because of the low contrast and the resulting yellowish dominant color. In this case, it is not useful to apply to the whole galactic plane image a single global transformation which maps the source intensities to the gray levels of the three channels, as we did in Figure 3. Therefore, to obtain the optimal scaling in each region of the final image, a "local stretching" and a "local color balance" procedure has been applied. The result is shown in the right panels of Figure 4, where we see many colors, high contrast, no dominant tint, and where plenty of features are clearly visible.

Of course, the result of a local process depends on the adopted "local" scale due that a wide scale improves the visibility of large features, while a small scale improves tiny details. So we apply this local enhancement to a set of spatial scales, and then average them in the final image. This method accomplish our definition that *"the best colors and brightness transformations are those that improves the features visibility at any scale"*.

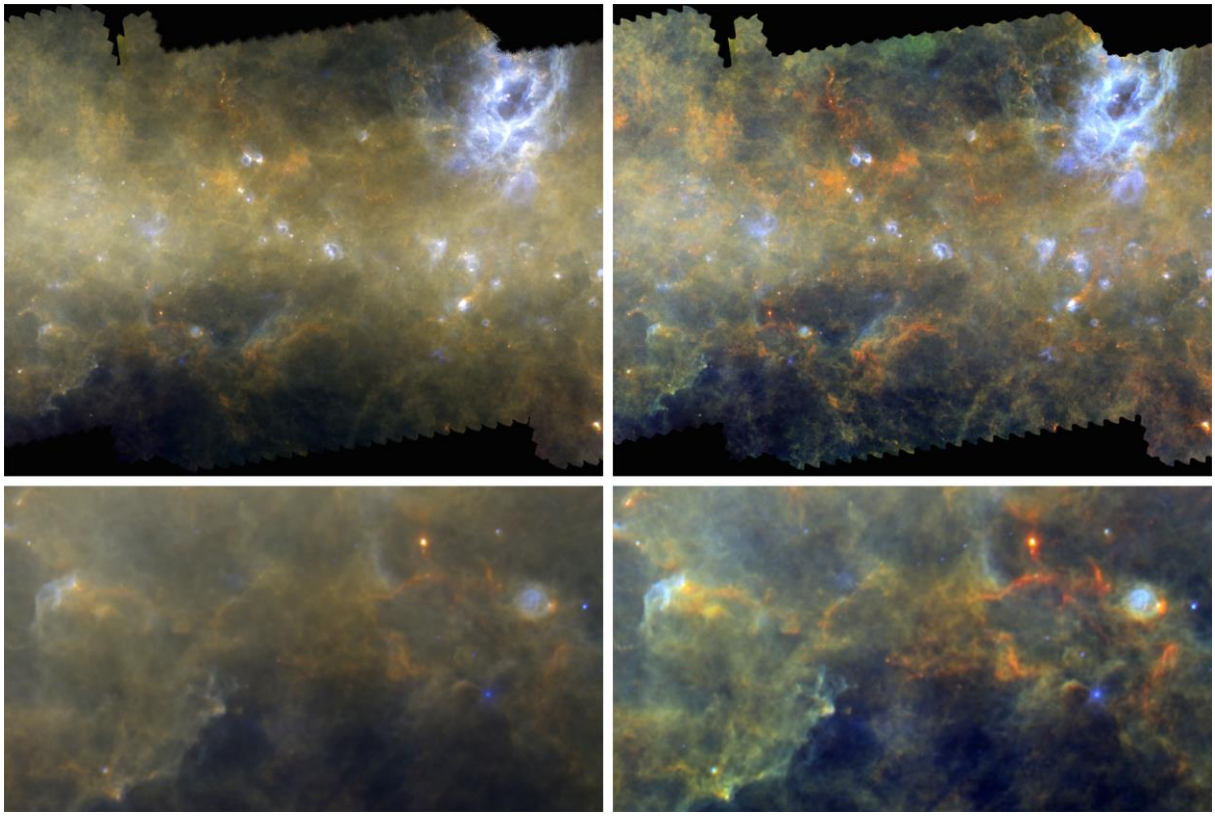

Figure 4: Top-left: Sub-region extracted from processing stage of bottom stripe in Figure 3, compared to the same area extracted from a multi-scale histogram and color local processing (top-right). Bottom panels: full resolution enlargements of top panels.

To implement such "multi-scale local processing", we defined a vector of spatial scales where each dimension w_i is half the dimension of previous scale, ranging between the ~4000 pixels width of the panorama down to the lower limit of 4 pixels, in power of two. For each scale, channel, and pixel the histogram stretching is locally computed on a square box with the current scale size, assigning the result to the central pixel. In practice, the image is stretched between an image of local minima and an image of local maxima (Figure 5), computed, respectively, by a smoothed erosion and a smoothed dilation morphological image operators applied at the considered scale.

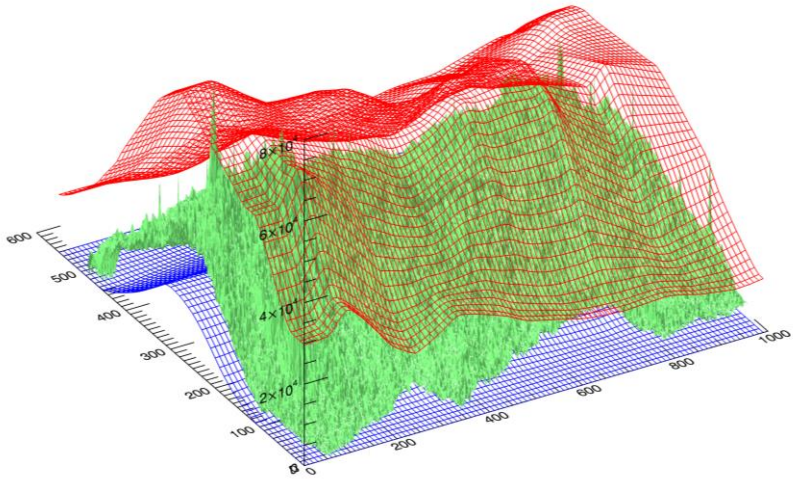

Figure 5: Local stretching method plot: for each spatial scale, the image (green) is normalized between an image of local maxima (red) and an image of local minima (blue) computed at the considered spatial scale by means of morphological image operators.

In detail, the histogram stretched image $\boldsymbol{H_i}$ for the $\boldsymbol{i^{th}}$ spatial scale, for each channel, can be written as:

$$H_i = \frac{I - I_i^{\min}}{I_i^{\max} - I_i^{\min}} \tag{1}$$

where $\boldsymbol{I^{min}}$ and $\boldsymbol{I^{max}}$ are the images containing, in each pixel, the minimum and maximum value of the image $\boldsymbol{I}$ within a box $\boldsymbol{b_i}$ of the current scale size $\boldsymbol{w_i}$ centered on that pixel. We can represent their composition as follows:

$$\begin{aligned} I_i^{\min} &= \left(I \ominus b_i\right) \otimes b_i \\ I_i^{\max} &= \left(I \oplus b_i\right) \otimes b_i \end{aligned} \tag{2}$$

where the Θ and $\oplus$ represents the erosion and dilation morphological operators, with a structuring element equal to the current box, and $\otimes$ is the convolution with the current box.

After local stretching, a local color balance is applied on the same set of spatial scales. In practice, a "gamma" transfer function is applied to each channel, i.e. the normalized channel levels are powered to the logarithmic ratio between the smoothed average of all channels and the smoothed channel itself. The $\boldsymbol{j^{th}}$ channel of the resulting $\boldsymbol{i^{th}}$ spatial scale rgb image $\boldsymbol{R_i}$ is:

$$R_{i,j} = H_{i,j}^{\log\left(\overline{H_{i,j} \otimes b_i}\right) / \log\left(H_{i,j} \otimes b_i\right)} \tag{3}$$

where the overbar indicates the average of the three channels and $\boldsymbol{j}$ is the channel index.

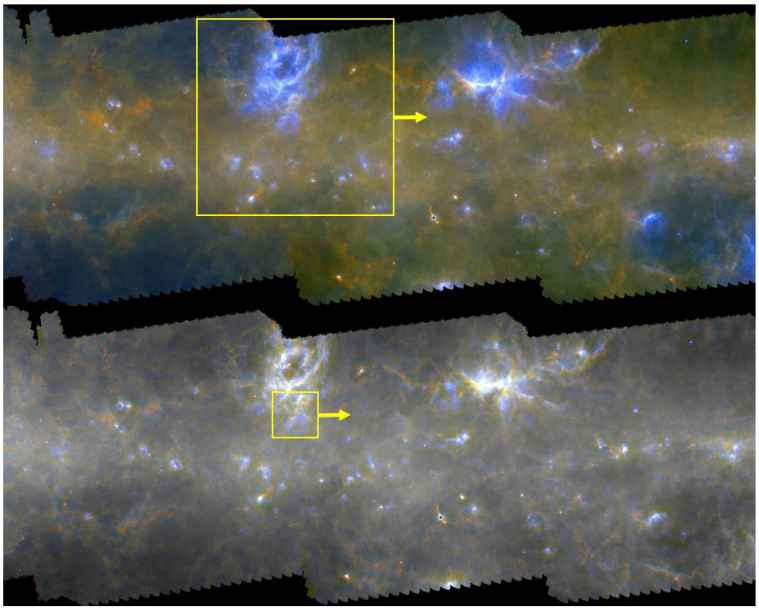

Figure 6: Example showing local processing: top image is the result of a wide-scale running box, enhancing distant color differences; bottom image is the result of a small-scale running box, enhancing adjacent color differences.

Such process produces an optimal image at each spatial scale. In Figure 6 two examples of the effects of the local stretching application are provided: a wide-scale running box improves the visibility of wide features differences, but does not improve the visibility of tiny details, while a small-scale box does the opposite.

The last step of the procedure is the production of a unique image $\boldsymbol{Z}$ by averaging all the $\boldsymbol{R_i}$ layers with weights proportional to their scales:

$$Z = \frac{\sum_i w_i R_i}{\sum_i w_i} \tag{4}$$

where $\boldsymbol{w_i}$ are the scales that we choose.

3.2 Artifact-free sharpening

To mitigate the blurring caused by the wide, and different, shapes of the point spread functions in the three bands (Figure 7, central panel) a final image sharpening function has been implemented.

The process of image sharpening, which means rising details contrast at pixel scale, is commonly done in digital photography by subtracting a smoothed image from the original, enhance this difference, and add it to the smoothing, a method called “unsharp masking”. This method however produces ringing artifacts around sharp edges, yielding halos and gradient reversals until a distance equal to the smoothing size, which on our images produces an ugly “hammered” appearance that is even worse than the blurring itself, as clearly shown in the left panel of Figure 7.

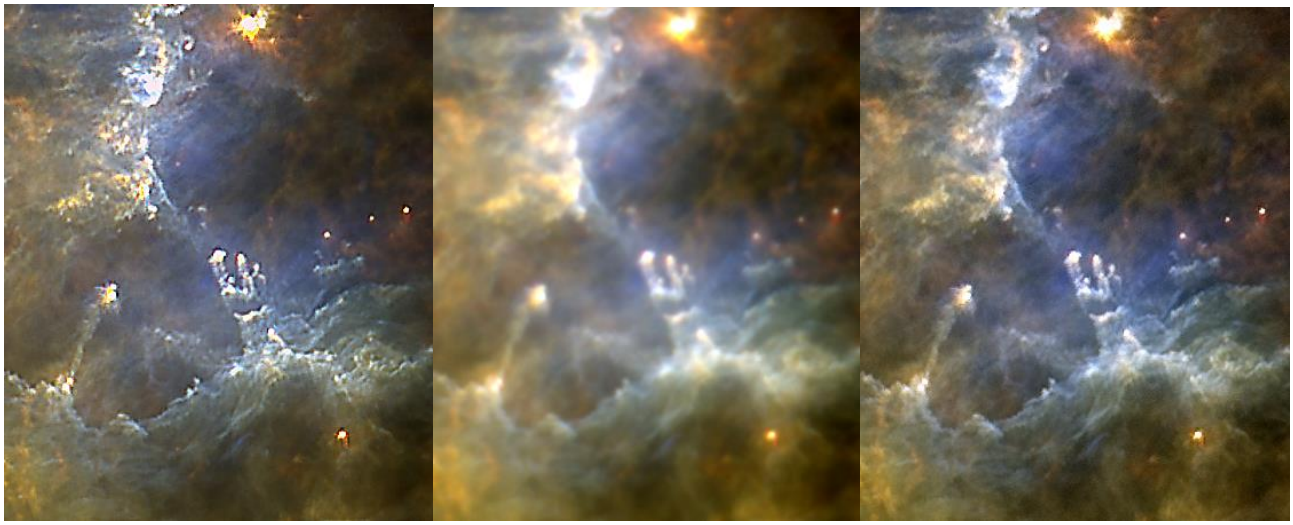

Figure 7: Center: full resolution enlargement of the well-known "pillars of creation" region of the Aquila Nebula, M16, extracted from the galactic plane image, after the processing stage of adaptive color balance and stretching described in Sec. 3.1. The image shows a noticeable blurring of the details with respect to its pixel scale. Left: details enhancements by unsharp masking results in artifact gradient reversals at the edges of all features. Right: artifact-free improved sharpness obtained by application of the described multi-scale and edge-preserving contrast enhancement, which reveals pixel scale details.

To avoid these effects, an alternative method has been adopted, i.e. the Edge-Preserving Contrast Enhancement method of Farbman et al. 2008[12]. The implemented IDL procedure included therefore an external call to the MATLAB scripts they provide, suitably conditioned for piecewise operation on our image frames. This algorithm computes an edge-preserving image smoothing by means of a weighted least square technique that may be viewed as a compromise between two contradictory goals: given the image $\boldsymbol{Z}$ in input the method seeks a new image $\boldsymbol{Z'}$, which is both as close as possible to $\boldsymbol{Z}$, and as smooth as possible everywhere, except across significant gradients in $\boldsymbol{Z}$. After some experiments, we found the set of parameters that produces the best focus improvement for our kind of images, revealing artifact-free details at pixel scale hardly visible in the blurred input, as well demonstrated by the right panel of Figure 7.

4. FINAL PROCESSING AND RESULTS

All the image processing done until this point works in a semi-automatic way. To this we finally add a manual interactive process, done with a common photo-editing tool, with the purely aesthetic aim of improving the color saturation, choosing the overall hue and contrast level of the final image, and apply a noise reduction filter in the faintest regions, if needed.

The resulting high-resolution panorama of the 130° central part of the Hi-GAL panorama, between $60° \geq l \geq -70°$, is shown in a folded version in Figure 8, but can be viewed at full resolution in the interactive on-line version[13] that we made publicly available with the recent release of the Hi-Gal mosaics and compact source catalog[14].

Finally, Figure 9 to Figure 16 present the most beautiful and meaningful snapshots of the star forming regions included in this stunning panorama.

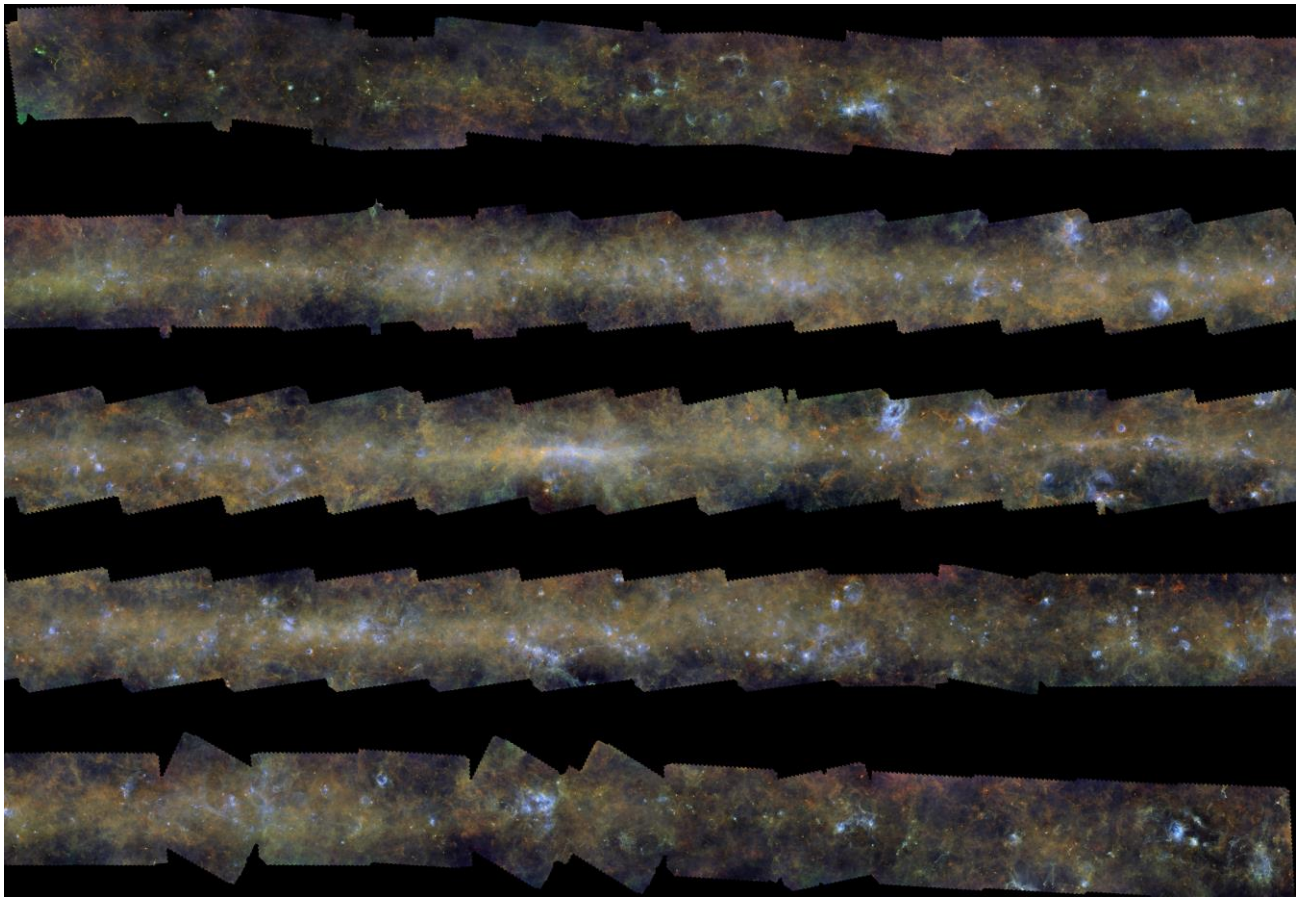

Figure 8: The 130° stripe of the central region of the Hi-GAL panorama, between 60° ≥ l ≥ -70°, is folded here in five contiguous pieces. The Galactic Center is soon recognizable in the central stripe, with many bright star forming regions, in blue-white color, and lots of cold filaments, in orange-red color.

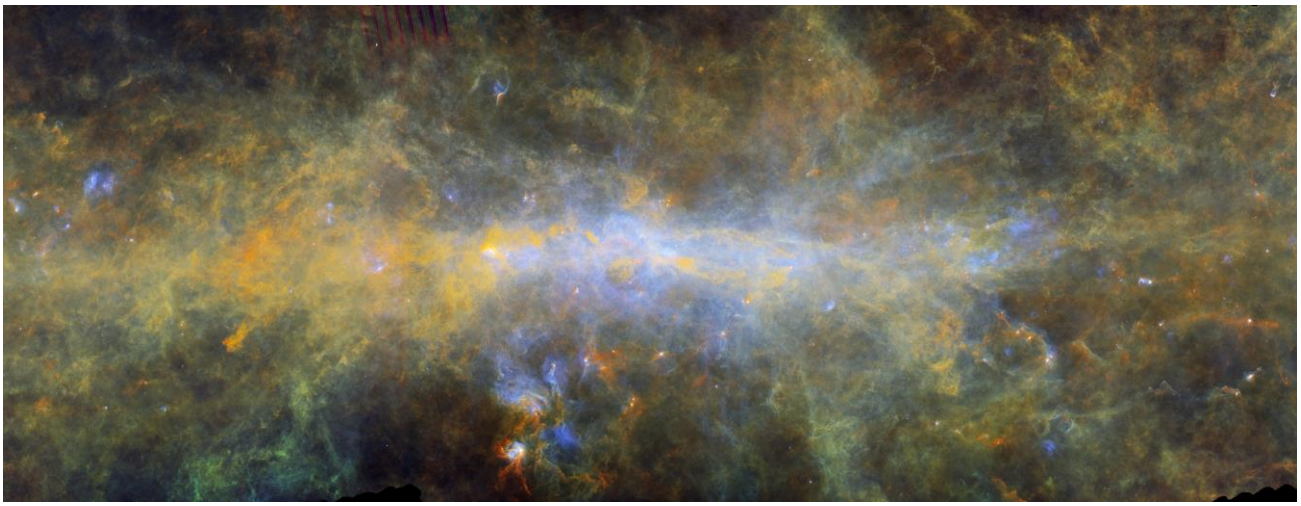

Figure 9: Galactic Center region.

Figure 10: The RCW106 Giant Molecular Cloud.

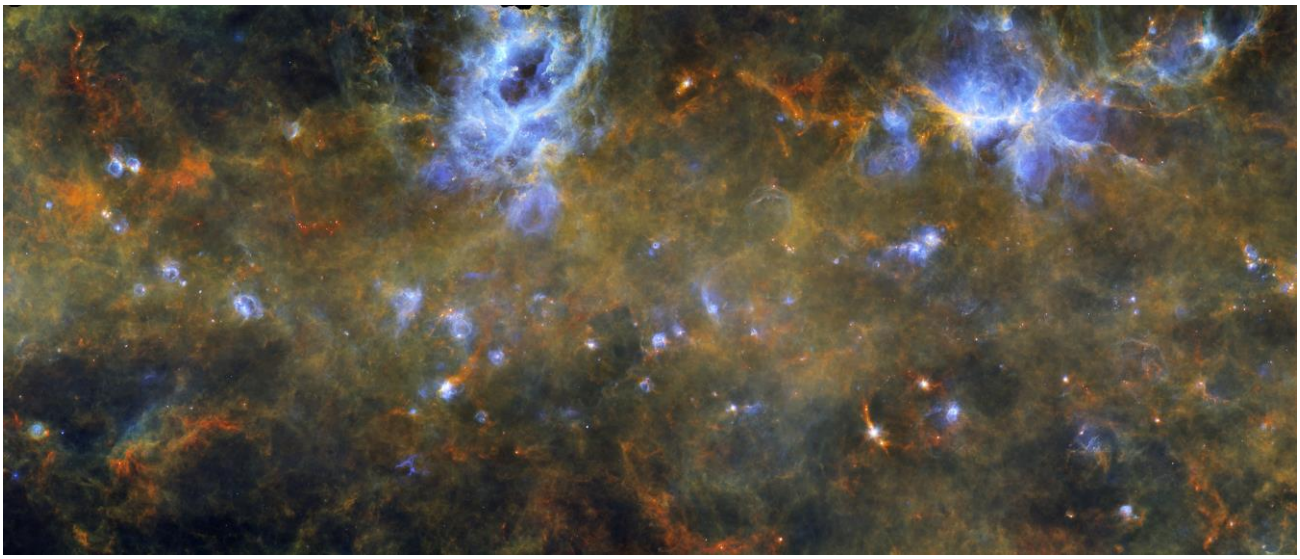
Figure 11: The nebulae NGC 6357 (Cat's pow), on the left, and NGC 6334 (War and Piece), on the right.

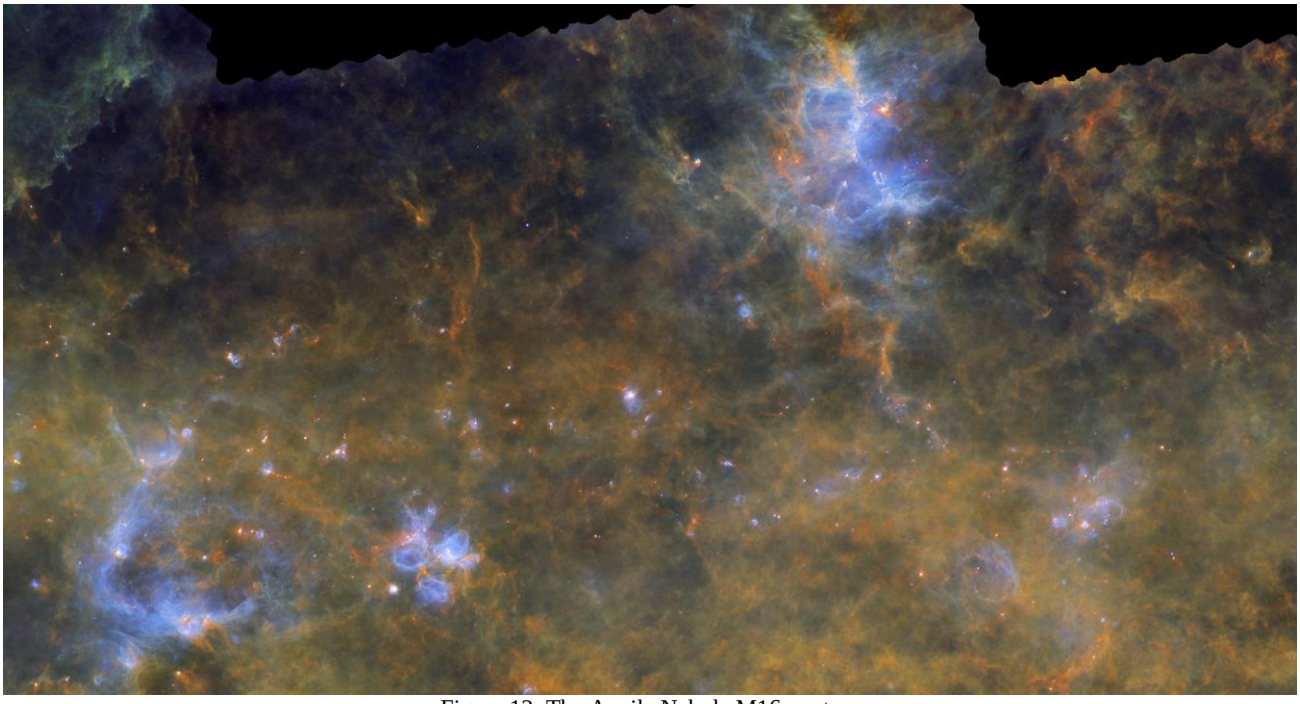

Figure 12: The Aquila Nebula M16, on top.

Figure 13: The L30 nebula complex.

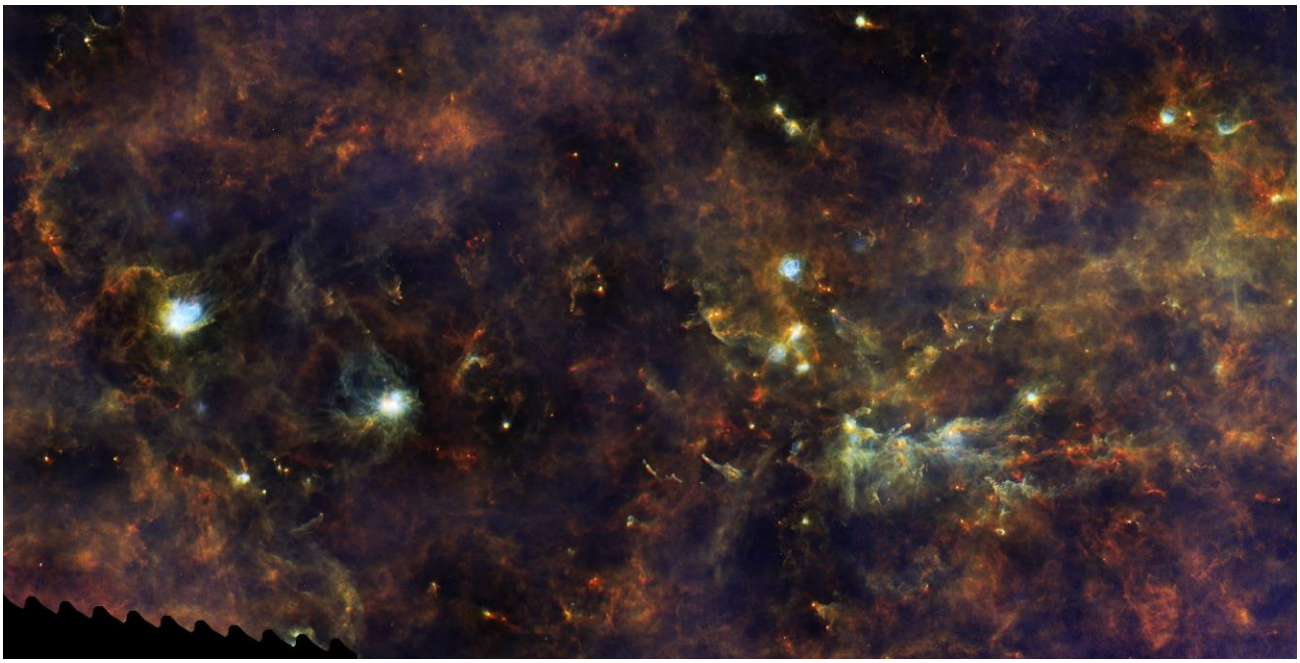

Figure 14: the Vulpecula OB1 region.

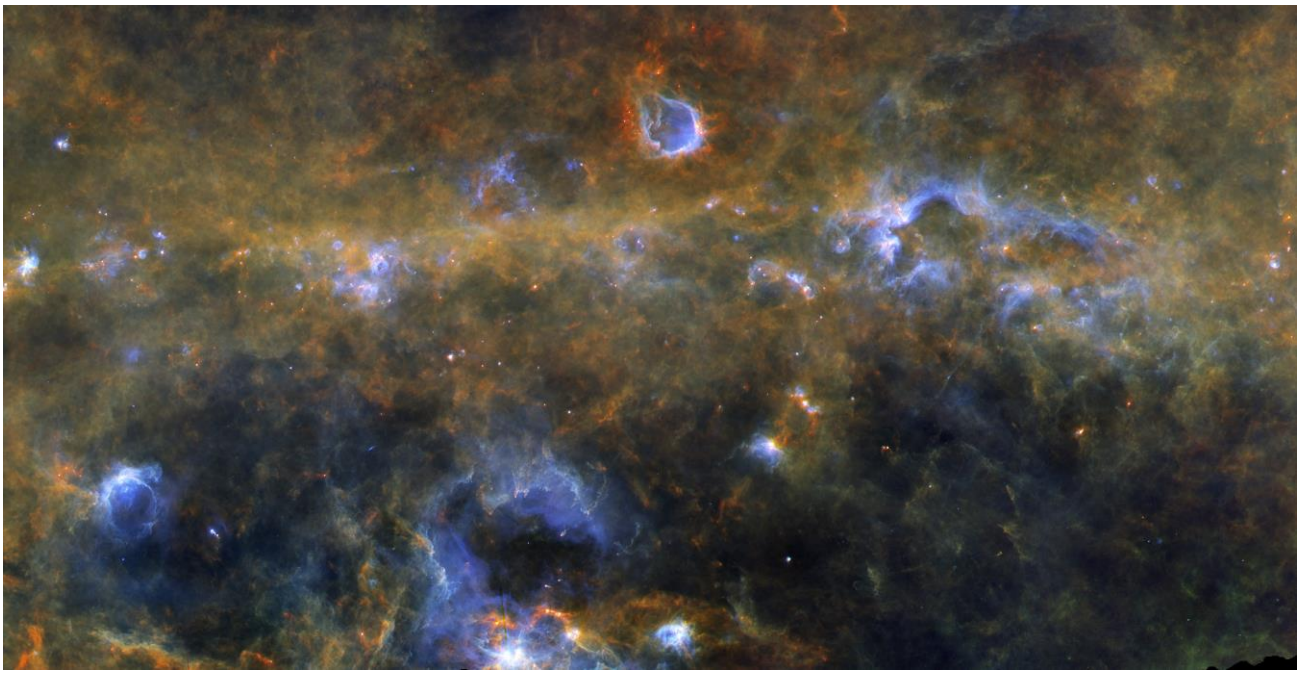

Figure 15: The RCW120 galactic bubble.

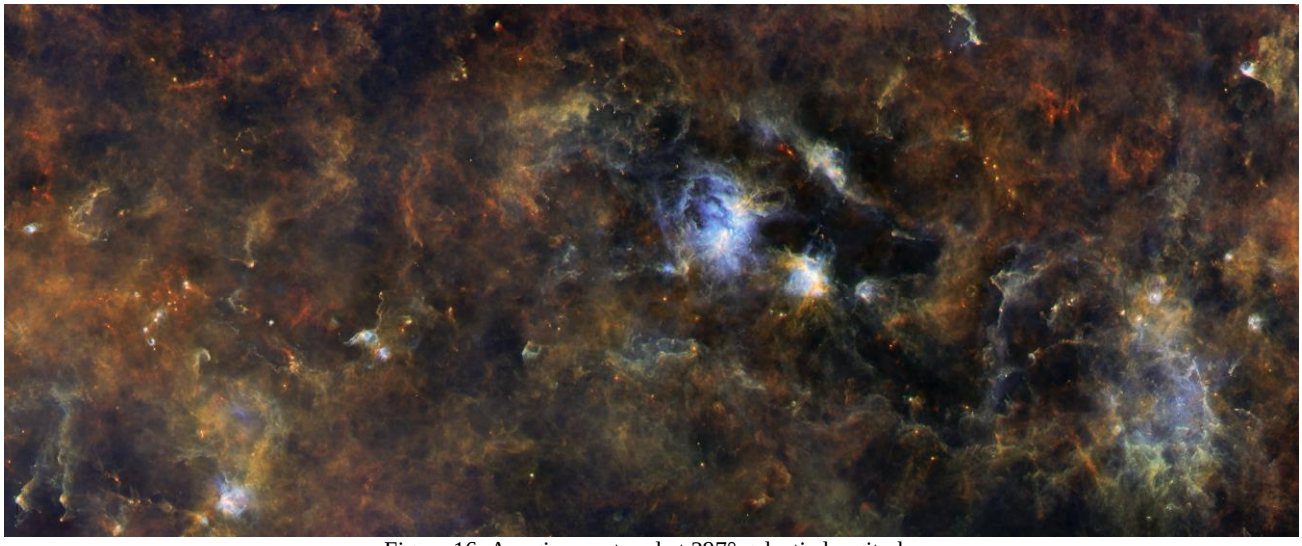

Figure 16: A region centered at 297° galactic longitude.

REFERENCES

[1] Pilbratt, G., Riedinger, J. R., Passvogel, T., et al., "Herschel Space Observatory", A&A, 518, L1, (2010)
[2] Molinari, S., Swinyard, B., Bally, J., et al., "Clouds, filaments, and protostars: The Herschel[*] Hi-GAL Milky Way", A&A, 518, L100, (2010)
[3] Poglitsch, A., Waelkens, C., Geis, N., et al., A&A, 518, L2, (2010)
[4] Griffn, M. J., Abergel, A., Abreu, A., et al., A&A, 518, L3, (2010)
[5] Traficante, A., Calzoletti, L., Veneziani, M., et al., MNRAS, 416, 2932, (2011)
[6] Piazzo, et al., MNRAS 447, issue 2, (2015)
[7] Bernard, et al., A&A 518, L88, (2010)
[8] Pence, W. D., Chiappetti, L., Page, C. G., et al., "Definition of the Flexible Image Transport System (FITS), version 3.0", A&A, 524, (2010)
[9] Exelis Visual Information Solutions, Inc., "IDL, Interactive Data Language", http://www.harrisgeospatial.com/ProductsandSolutions/GeospatialProducts/IDL/Language.aspx
[10] AWare Systems, "The BigTIFF File Format Proposal", http://www.awaresystems.be/imaging/tiff/bigtiff.html
[11] KrPano Panorama Viewer, http://krpano.com/
[12] Farbman, Z., Fattal, R., Lischinski, D., Szeliski, R., "Edge-Preserving Decompositions for Multi-Scale Tone and Detail Manipulation", Journal ACM Transactions on Graphics, Proceedings of ACM SIGGRAPH 2008, Volume 27, Issue 3, (2008)
[13] Li Causi, G., http://visivo.oact.inaf.it/vialactea/openlayers.html
[14] Molinari, S., Schisano, E., Elia, D., et al., "Hi-GAL, the Herschel infrared Galactic Plane Survey: photometric maps and compact source catalogues", arXiv:1604.05911, (2016)
[15] Molinari, S., et al, "A 100pc elliptical and twisted ring of cold and dense molecular clouds revealed by Herschel around the galactic center", AJ Letters, 735:L33, (2011)